

Communication

# Thermal Kinetics of Monocationic and Dicationic Pyrrolidinium-Based Ionic Liquids

Asyraf Hanim Ab Rahim<sup>1</sup>, Noraini Abd Ghani<sup>1,2,\*</sup>, Noorhafizah Hasanudin<sup>1</sup>, Normawati M. Yunus<sup>1,2</sup>  
and Ninna Sakina Azman<sup>1,2</sup>

<sup>1</sup> Centre of Research in Ionic Liquids, Universiti Teknologi PETRONAS, Seri Iskandar 32610, Perak, Malaysia; asyrafhanim92@gmail.com (A.H.A.R.); fiezah\_hfzh@yahoo.com (N.H.); normaw@utp.edu.my (N.M.Y.); ninna.azman@gmail.com (N.S.A.)

<sup>2</sup> Fundamental and Applied Sciences Department, Universiti Teknologi PETRONAS, Seri Iskandar 32610, Perak, Malaysia

\* Correspondence: noraini.ghani@utp.edu.my

**Abstract:** This work presents an in-depth kinetic thermal degradation comparison between traditional monocationic and the newly developed dicationic ionic liquid (IL), both coupled with a bromide ( $\text{Br}^-$ ) anion by using non-isothermal thermogravimetric analysis. Thermal analyses of 1-butyl-1-methylpyrrolidinium bromide  $[\text{C}_4\text{MPyr}][\text{Br}]$  and 1,4-bis(1-methylpyrrolidinium-1-yl)butane dibromide  $[\text{BisC}_4\text{MPyr}][\text{Br}_2]$  were conducted at a temperature range of 50–650 °C and subjected to various heating rates, which are 5, 10, 15, 20 and 25 °C/min. Thermogravimetric analysis revealed that dicationic IL,  $[\text{BisC}_4\text{MPyr}][\text{Br}_2]$  is less thermally stable compared to monocationic  $[\text{C}_4\text{MPyr}][\text{Br}]$ . A detailed analysis of kinetic parameters, which are the activation energy ( $E_a$ ) and pre-exponential factor ( $\log A$ ), was calculated by using Kissinger-Akahira-Sunose (KAS), Flynn-Wall-Ozawa (FWO) and Starink. This study revealed that the average  $E_a$  and  $\log A$  of  $[\text{BisC}_4\text{MPyr}][\text{Br}_2]$  are lower than  $[\text{C}_4\text{MPyr}][\text{Br}]$ , which may be contributed to by its low thermal stability. Conclusively, it proved that the  $E_a$  and  $\log A$  of ILs are strongly related to the thermal stability of ILs.

**Keywords:** ionic liquids; monocationic; dicationic; thermal kinetic; activation energy



**Citation:** Ab Rahim, A.H.; Abd Ghani, N.; Hasanudin, N.; Yunus, N.M.; Azman, N.S. Thermal Kinetics of Monocationic and Dicationic Pyrrolidinium-Based Ionic Liquids. *Materials* **2022**, *15*, 1247. <https://doi.org/10.3390/ma15031247>

Academic Editor: Anton Trnik

Received: 10 December 2021

Accepted: 8 January 2022

Published: 8 February 2022

**Publisher's Note:** MDPI stays neutral with regard to jurisdictional claims in published maps and institutional affiliations.



**Copyright:** © 2022 by the authors. Licensee MDPI, Basel, Switzerland. This article is an open access article distributed under the terms and conditions of the Creative Commons Attribution (CC BY) license (<https://creativecommons.org/licenses/by/4.0/>).

## 1. Introduction

The first ever ionic liquids (ILs) were founded by Paul Walden in 1914, as he discovered ethyl ammonium-nitrate  $[\text{EtNH}_3][\text{NO}_3]$ , which had a melting point less than 12 °C [1]. This discovery has become a foundation that inspires researchers to synthesize various ILs, such as 1-ethylpyridinium bromide-aluminium chloride  $[\text{C}_2\text{Py}][\text{Br-AlCl}_3]$ , 1-butylpyridinium chloride-aluminium chloride  $[\text{C}_4\text{Py}][\text{Cl-AlCl}_3]$  and 1-butyl-3-methylimidazolium chloride [2–4]. Basically, ILs are a molten salt consisting of cations and anions and have a melting point lower than 100 °C [5]. In the late 20th century, works related to ILs demonstrated increasing trends, mainly due to its unique properties, such as high thermal stability, wider liquidous range and negligible vapor pressure [6]. Apart from that, the properties of ILs, namely, thermal stability, viscosity, hydrophobicity and conductivity, can be changed according to the application of interest, due to the availability of various cation and anion combinations [7].

The thermal stability of ILs is an important parameter that should be considered before ILs are applied to specific application. Apart from the academic perspective, the thermal stability of ILs is crucial in some applications involving high temperature, such as transesterification and dissolution. According to Xu and Cheng, the thermal stability studies of ILs are usually conducted by using UV-Vis spectroscopy, flame ionization detection (FID) and mass spectrometry (MS) [8]. Nevertheless, the most popular technique involves the determination of onset temperature ( $T_o$ ), which is measured by using a thermogravimetric analyzer (TGA) [9,10]. Through TGA, an isoconversional kinetic study can be conducted due to



## 2.2. Instrumentations

### 2.2.1. Structural Characterization

$^1\text{H}$  and  $^{13}\text{C}$  characterizations of ILs were recorded on a Bruker Advance III (500MHz) Nuclear Magnetic Resonance (NMR) spectrometer (Bruker, Billerica, MA, USA) using deuterated solvent,  $\text{D}_2\text{O}$ . About 80  $\mu\text{L}$  of the IL sample was added into a NMR tube containing 550  $\mu\text{L}$   $\text{D}_2\text{O}$ . The measurement was conducted at room temperature and the chemical shift was reported in parts per million (ppm) with TMS as an internal standard. The multiplicities were abbreviated as s = singlet, d = duplet, t = triplet and m = multiplet.

### 2.2.2. Elemental Analysis

The percentage of carbon (C), hydrogen (H) and nitrogen (N) in ILs were analyzed by using CHNS Elementar Vario Micro Cube with infrared analyzer (Elementar Analysensysteme GmbH, Langenselbold, Germany). About 2.0 mg of the IL sample was weighed by a highly precise balance in aluminium foil and sealed in a silver capsule. The sample was loaded in an autosampler to be analyzed. Before the analysis, the instrument was calibrated by using sulfonamide. The measurement was conducted at 1000  $^\circ\text{C}$  and the reduction furnace temperature was 650  $^\circ\text{C}$ . Helium was used as the carrier gas.

### 2.2.3. Thermal Pyrolysis of ILs

The thermogravimetric analysis (TG) of the ILs was measured using STA 6000 from Perkin Elmer, Waltham, MA, USA. In this work, about 5.0 mg of sample was weighed in a crucible pan and placed on the sample holder. The measurement was conducted at five different heating rates, which are 5, 10, 15, 20 and 25  $^\circ\text{C}/\text{min}$ , to study the degree of pyrolysis in the temperature range of 50–650  $^\circ\text{C}$  under 20 mL/min nitrogen flow. The condition for thermal pyrolysis was selected based on a preliminary analysis on the IL's degradation, also based on the method suggested by Masri et al. and Meng et al. [26,27]. In this study, the thermal analysis for kinetic pyrolysis was done twice under the same conditions to verify the reliability of the results.

## 2.3. Experimental

### 2.3.1. Synthesis of Monocationic IL; 1-butyl-1-methylpyrrolidinium bromide [ $\text{C}_4\text{MPyr}$ ][Br]

The synthesis of monocationic [ $\text{C}_4\text{MPyr}$ ][Br] was conducted based on the method suggested by Burrell and co-workers [24]. An equal molar of 1-bromobutane (8.05g, 0.059 mole) was slowly added into a round bottom flask containing methylpyrrolidine (5 g, 0.059 mole) that was stirred at 150 rpm. The reaction was conducted under a solventless condition. The mixture was refluxed at 40  $^\circ\text{C}$  for 24 h. A total of 15 mL of diethyl ether was added into the resulting product and the mixture was moderately shaken to remove unreacted reactants. The step was repeated for three times before the resulted clear yellowish liquid, then was dried in a vacuum oven for 24 h (89.9%).  $^1\text{H}$  NMR (500 MHz,  $\text{D}_2\text{O}$ )  $\delta$  = 1.81 (m, 4H,  $\text{CH}_2$ ), 2.13 (s, 8H,  $\text{CH}_2\text{-N}$ ), 2.97 (s, 6H,  $\text{CH}_3$ ), 3.33 (t, 4H,  $\text{CH}_2\text{-N}$ ), 3.45 (m, 8H,  $\text{CH}_2$ ). Theoretical calculation (%): C, 48.66; H, 9.07; N, 6.30, Experimental: C, 48.24; H, 9.13; N, 6.45.

### 2.3.2. Synthesis of Dicationic IL; 1,4-bis(1-methylpyrrolidinium-1-yl)butane dibromide [ $\text{BisC}_4\text{MPyr}$ ][ $\text{Br}_2$ ]

The synthesis of dicationic [ $\text{BisC}_4\text{MPyr}$ ][ $\text{Br}_2$ ] was conducted based on the method provided by Montalbán et al. [25]. An equal molar of 1,4-dibromobutane (10.8 g, 0.05 mole) was slowly added into a round bottom flask containing a mixture of methylpyrrolidine (4.3 g, 0.05 mole) and 2-propanol and stirred at 150 rpm. The mixture was refluxed at a temperature of 70  $^\circ\text{C}$  for 24 h. Then, 2-propanol was evaporated in vacuo, resulting in highly viscous dark brown IL. The resulting IL was washed with 15 mL diethyl ether for three times before being dried under a vacuum to yield a solid product (86.0%).  $^1\text{H}$  NMR (500 MHz,  $\text{D}_2\text{O}$ )  $\delta$  = 1.97 (t, 4H), 2.24 (s, 8H), 3.084 (s, 6H), 3.08 (s, 6H), 3.40 (t, 4H), 3.58 (m, 8H). Theoretical calculation (%): C, 43.54; H, 7.83; N, 7.25. Experimental: C, 43.62; H, 8.0; N, 7.65.

### 2.4. Kinetic Thermal Decomposition

The kinetics of the mono and di-IL decomposition reaction was determined by using the Starink, KAS and FWO methods. These three methods were selected as they are frequent p(y)-isoconversion methods, which allows the measurement of kinetic parameters,  $E_a$  and  $\log A$  for at different heating rates. Each method produced a thermokinetic based on equations by KAS, FWO and Starink, as depicted in Equations (1)–(3), respectively [26].

$$\ln\left(\frac{\beta}{T^2}\right) = \ln\left(\frac{AR}{E_a g(\alpha)}\right) - \frac{E_a}{RT} \quad (1)$$

$$\ln\beta = \ln\left(\frac{AE_a}{Rg(\alpha)}\right) - 5.331 - \frac{1.052E_a}{RT} \quad (2)$$

$$\ln\left(\frac{\beta}{T^{1.92}}\right) = \ln\left(\frac{AR^{0.92}}{g(\alpha)E_a^{0.92}}\right) - 0.312 - \frac{1.008E_a}{RT} \quad (3)$$

where  $\beta$  represents heating rates,  $T$  is the absolute temperature,  $g(\alpha)$  is a function conversion factor,  $A$  is the pre-exponential factor,  $R$  is the ideal gas constant of 8.314 J/mol, while  $E_a$  is the activation energy. The calculation to obtain  $E_a$  and  $\log A$  is performed by using the average temperature obtained in each  $\alpha$  value, as provided in the supplementary data.

## 3. Results and Discussions

### 3.1. Thermal Decomposition Analysis

In this work, the thermal stability of [C<sub>4</sub>MPyr][Br] and [BisC<sub>4</sub>MPyr][Br<sub>2</sub>] was reported in term of onset temperature ( $T_o$ ) and decomposition temperature ( $T_{max}$ ).  $T_o$  is an intersection that exists between the baseline and the tangent of sample weight vs. temperature, whereas  $T_{max}$  is the temperature in which the maximum weight loss of the sample was recorded [10]. The thermogravimetric (TG) curves of mono- [C<sub>4</sub>MPyr][Br] and dicationic [BisC<sub>4</sub>MPyr][Br<sub>2</sub>] ILs were compared in Figure 2a,c. Meanwhile, the  $T_o$  for both ILs at heating rates of 5 to 25 °C/min are shown in Table 1. Based on Table 1, it is demonstrated that the  $T_o$  for [C<sub>4</sub>MPyr][Br] is higher than [BisC<sub>4</sub>MPyr][Br<sub>2</sub>]. Generally, this indicates a better thermal stability of mono-[C<sub>4</sub>MPyr][Br] compared to [BisC<sub>4</sub>MPyr][Br<sub>2</sub>]. This result is opposed to studies performed by Bender et al. and Fareghi et al., in which they reported a better thermal stability for dicationic imidazolium-based ILs [28,29].

The difference in the thermal behavior of [BisC<sub>4</sub>MPyr][Br<sub>2</sub>] compared to other dicationic ILs could be caused by its chemical structure, which consists of heterocyclic non-aromatic pyrrolidinium instead of aromatic imidazolium and pyridinium. Theoretically, the improvement of thermal stability for dicationic ILs with aromatic heterocyclic structures is due to the delocalization and the presence of  $\pi$  bonds in its entire ring system. Therefore, the presence of the double aromatic in dicationic ILs will significantly improve their thermal stability. However, for ILs in this study, the presence of two weak non-aromatic heterocyclic pyrrolidinium rings may contribute to the low thermal stability of [BisC<sub>4</sub>MPyr][Br<sub>2</sub>]. Other than that, the presence of the more powerful nucleophile Br<sup>-</sup> in [BisC<sub>4</sub>MPyr][Br<sub>2</sub>] compared to [C<sub>4</sub>MPyr][Br] may also cause the decrease in the thermal stability of [BisC<sub>4</sub>MPyr][Br<sub>2</sub>]. At 25 °C, the density of mono-[C<sub>4</sub>MPyr][Br] is 1.1997 cm<sup>-3</sup>, which is larger than dicat-[BisC<sub>4</sub>MPyr][Br<sub>2</sub>], with a density value of 1.4726 cm<sup>-3</sup>. This result was in line with work conducted by Shirota and co-workers, in which ILs with high densities possessed better thermal stability compared with ILs with low densities [16].

However, unlike [C<sub>4</sub>MPyr][Br], with a single peak at its derivative thermogravimetric (DTG) curve, the DTG curve of [BisC<sub>4</sub>MPyr][Br<sub>2</sub>] displays the presence of several peaks, which suggests that multiple stages have occurred in the decomposition process. However, only the highest peak in DTG was selected for further analysis [30]. It is revealed that the  $T_{max}$  of both ILs also reflects the same result as  $T_o$ , where the  $T_{max}$  for [C<sub>4</sub>MPyr][Br] and [BisC<sub>4</sub>MPyr][Br<sub>2</sub>] are in the range of 283–294 °C and 205–254 °C, respectively. In addition, as shown in Table 1, an increase in heating rates increased the  $T_o$  and  $T_{max}$  of ILs, which is in

agreement with the data reported in the previous literature [20]. This is due to the increase of heat supply into the system, as when the heating rate increased, faster chemical reaction kinetics were caused [31].

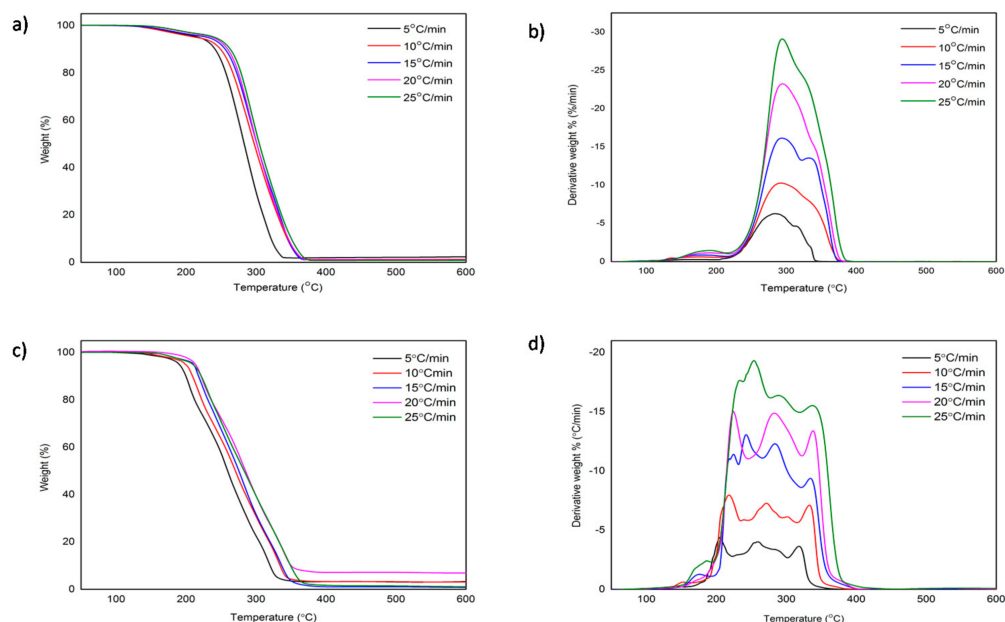


**Figure 2.** The TG and DTG curves for (a,b)  $[C_4MPyr][Br]$  and (c,d)  $[BisC_4MPyr][Br_2]$  at heating rate of 5–25 °C/min.

**Table 1.**  $T_o$  and  $T_{max}$  at different heating rates.

Heating Rate/ $^{\circ}C\ min^{-1}$	$[C_4MPyr][Br]$		$[BisC_4MPyr][Br_2]$	
	$T_o$ ( $^{\circ}C$ )	$T_{max}$ ( $^{\circ}C$ )	$T_o$ ( $^{\circ}C$ )	$T_{max}$ ( $^{\circ}C$ )
5	$255 \pm 10$	$297 \pm 20$	$191 \pm 1$	$208 \pm 3$
10	$253 \pm 2$	$292 \pm 1$	$201 \pm 4$	$218 \pm 2$
15	$259 \pm 1$	$293 \pm 1$	$206 \pm 3$	$237 \pm 7$
20	$265 \pm 2$	$290 \pm 5$	$206 \pm 3$	$236 \pm 14$
25	$265 \pm 3$	$293 \pm 1$	$213 \pm 4$	$251 \pm 5$

In the meantime, although there is a difference between the DTG pattern of  $[C_4MPyr][Br]$  and  $[BisC_4MPyr][Br_2]$ , a similar pattern of behavior of the TG and DTG curves was observed for each individual IL, regardless of the different heating rates. This is attributed to the similar decomposition mechanism possessed by each ILs. Cao and Mu stated that the degradation of ILs consists of decomposition and evaporation processes [10]. In the decomposition stage, the formation of new substances occur due to the nucleophilic substitution reaction,  $SN_2$ , and is followed by the transformation of the sample into a gaseous state [32]. In the meantime, Patil et al. and Wooster et al. provided a detailed study on the mechanisms for ILs decomposition by analyzing pyrolysis products using mass spectrometry [33,34]. Generally, the thermal degradation mechanism of ILs mainly involved reverse Menshutkin reactions and Hofmann eliminations [34]. The attack of the nucleophilic  $Br^-$  anion towards the cation moiety led to the loss of alkyl substituents on the pyrrole ring. Meanwhile, at the side chain, Hofmann elimination may contribute to the formation of terminal alkenes and protonated anions [34]. Figure 3a,b demonstrates the postulated degradation mechanism of  $[C_4MPyr][Br]$  and  $[BisC_4MPyr][Br_2]$ .

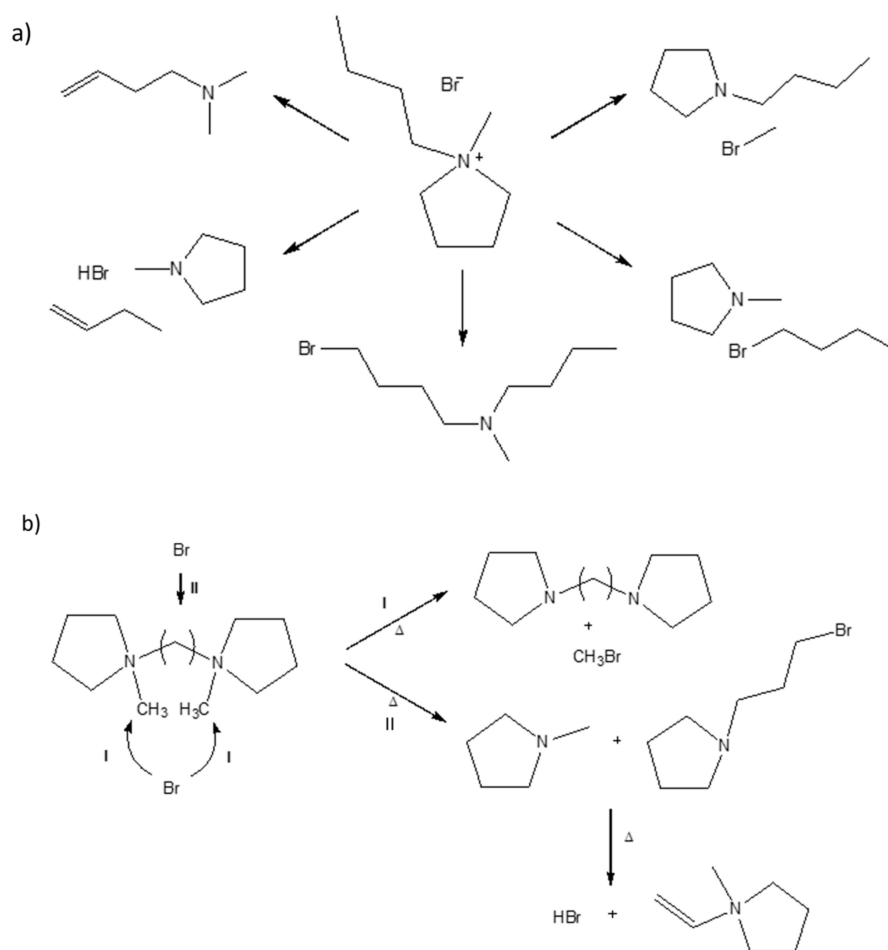


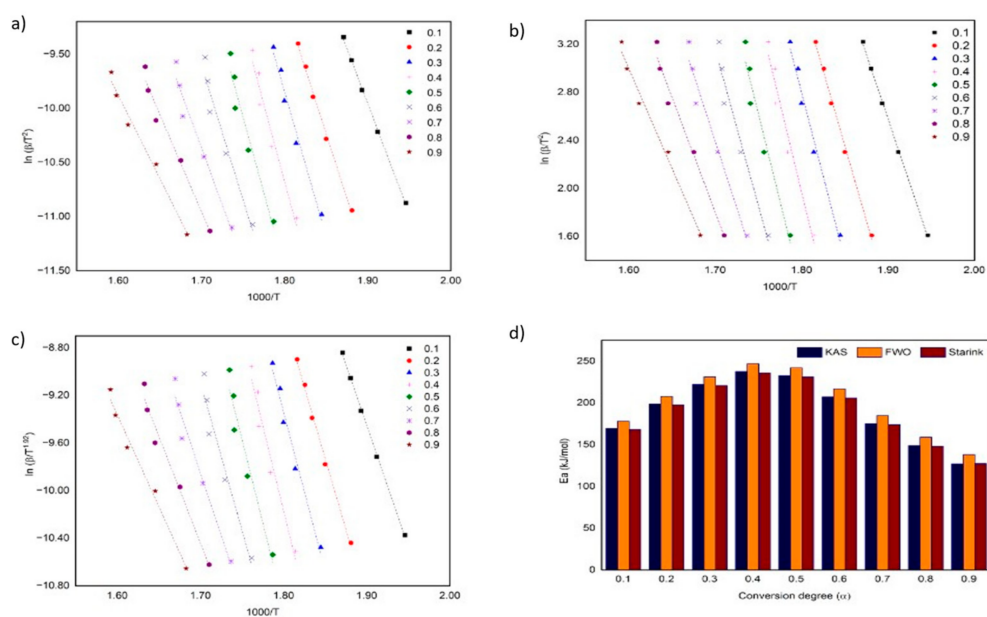
**Figure 3.** The postulated thermal degradation mechanism of (a)  $[C_4MPyr][Br]$  and (b)  $[BisC_4MPyr][Br_2]$ .

### 3.2. Kinetic of Thermal Decomposition

Theoretically, the kinetic of the thermal decomposition parameters for ILs can be calculated by using the TG and DTG approach. In this study, the kinetic parameters, namely,  $E_a$  and  $\log A$ , were calculated by using the TG approach, and it was determined based on a fraction conversion ( $\alpha$ ) by applying the KAS, FWO and Starink methods. Table 2 shows the correlation coefficient values ( $R^2$ ) of the three models exceeding 0.9, which indicates a high degree of linearity [31]. Figure 4 shows the thermokinetic plot for KAS, FWO and Starink, including  $E_a$ , for the monocationic IL,  $[C_4MPyr][Br]$ , at different  $\alpha$ . The average  $E_a$  of  $[C_4MPyr][Br]$ , as deduced by KAS, FWO and Starink, are  $191 \pm 38$ ,  $201 \pm 38$  and  $190 \pm 38$  kJ/mol, respectively. Moreover, the pre-exponential factor was presented in terms of the  $\log A$ , in which the values for KAS, FWO and Starink are  $17 \pm 4$ ,  $18 \pm 4$  and  $17 \pm 4$   $\text{min}^{-1}$ . According to Guida and co-workers, the slight difference in  $E_a$  and  $\log A$  values obtained is due to an improper approximation of temperature integration [35]. Based on Figure 4d, the three models show similar  $E_a$  trends from  $\alpha$  values of 0.1–0.9. An increasing trend of  $E_a$  was observed from  $\alpha$  values of 0.1–0.4 before it is reduced to a range of 0.5–0.9. The increase in  $E_a$  is due to the IL partial decomposition, which normally occurs in the beginning of the thermal process at low temperatures. Meanwhile, a reduction in  $E_a$  indicates the formation of intermediates due to the  $SN_2$  nucleophilic substitution reaction [26].

**Table 2.** Values of  $E_a$ ,  $\log A$  and  $R^2$  for  $[C_4MPyr][Br]$  and  $BisC_4MPyr][Br_2]$  at different fraction conversions.

Method	$\alpha$	$E_a$ (kJ/mol)		$\log A$ ( $\text{min}^{-1}$ )		$R^2$	
		$[C_4MPyr][Br]$	$[BisC_4MPyr][Br_2]$	$[C_4MPyr][Br]$	$[BisC_4MPyr][Br_2]$	$[C_4MPyr][Br]$	$[BisC_4MPyr][Br_2]$
KAS	0.1	169.28	139.79	15.79	14.03	0.9991	0.9837
	0.2	198.85	130.61	18.45	12.88	0.9953	0.9969
	0.3	222.03	142.82	20.51	13.89	0.9778	0.9885
	0.4	237.51	131.72	21.76	12.39	0.9544	0.9594
	0.5	232.59	118.52	21.03	10.80	0.941	0.9464
	0.6	207.17	113.32	18.41	10.06	0.9475	0.9585
	0.7	175.08	113.77	15.22	9.86	0.9601	0.9715
	0.8	148.97	124.55	12.63	10.58	0.9739	0.9739
	0.9	127.96	142.71	10.55	11.90	0.9846	0.956
FWO	0.1	177.99	147.83	15.77	14.10	0.9991	0.9894
	0.2	207.83	138.88	18.33	13.04	0.9957	0.9973
	0.3	231.19	151.35	20.30	14.00	0.9794	0.9898
	0.4	246.81	140.53	21.51	12.60	0.9576	0.9642
	0.5	242.04	127.59	20.81	11.12	0.9452	0.9535
	0.6	216.76	122.63	18.30	10.43	0.9518	0.9645
	0.7	184.85	123.34	15.27	10.25	0.9640	0.9757
	0.8	158.92	134.41	12.83	10.92	0.9770	0.9776
	0.9	138.12	152.87	10.90	12.16	0.9868	0.9616
Starink	0.1	168.28	139.00	16.83	15.07	0.9991	0.9837
	0.2	197.62	129.91	19.19	13.63	0.9953	0.9969
	0.3	220.63	142.02	21.06	14.46	0.9779	0.9885
	0.4	236.00	131.02	22.18	12.84	0.9545	0.9596
	0.5	231.13	117.93	21.37	11.15	0.9412	0.9467
	0.6	205.90	111.14	18.66	12.65	0.9477	0.9588
	0.7	174.08	113.25	15.42	10.07	0.9603	0.9717
	0.8	148.18	123.96	12.78	10.73	0.9741	0.9741
	0.9	127.35	141.97	10.65	15.07	0.9847	0.9563

**Figure 4.** Thermokinetic plot using (a) KAS, (b) FWO, (c) Starink method and (d) the  $E_a$  profile for  $[C_4MPyr][Br]$ .

In the meantime, Figure 5 shows the kinetic plot and  $E_a$  profile for  $[BisC_4MPyr][Br_2]$ . The average  $E_a$  for KAS, FWO and Starink are  $129 \pm 12$ ,  $138 \pm 12$  and  $128 \pm 12$  kJ/mol,

respectively. Based on Figure 4d, the  $E_a$  trend of  $[\text{BisC}_4\text{MPyr}][\text{Br}_2]$  fluctuates as the  $\alpha$  value increases. A work by Masri and co-workers also revealed the same trend for their  $([\text{DABCODBS}][\text{HSO}_4]_2)$  and  $([\text{DABCODBS}][\text{CF}_3\text{SO}_3]_2)$ . It was suggested that the fluctuating trend of  $E_a$  happened due to the multi-step thermal decomposition process [26]. The average  $\log A$  values of  $[\text{BisC}_4\text{MPyr}][\text{Br}_2]$  are  $12 \pm 2$ ,  $14 \pm 2$  and  $12. \pm 1 \text{ min}^{-1}$ . Further analysis of the kinetic parameters of both ILs demonstrated that  $[\text{BisC}_4\text{MPyr}][\text{Br}_2]$  owns lower  $E_a$  and  $\log A$  values compared to  $[\text{C}_4\text{MPyr}][\text{Br}]$ . This could be related to the low thermal stability of  $[\text{BisC}_4\text{MPyr}][\text{Br}]$  compared to  $[\text{C}_4\text{MPyr}][\text{Br}]$ . Furthermore, the low  $E_a$  of  $[\text{BisC}_4\text{MPyr}][\text{Br}_2]$  suggested that it had a faster chemical reaction than  $[\text{C}_4\text{MPyr}][\text{Br}]$ . While the Starink and KAS method produced almost identical  $E_a$  and  $\log A$  values for both ILs, the  $E_a$  obtained by using FWO is slightly higher. The  $E_a$ ,  $\log A$  and  $R^2$  values for both ILs were presented in Table 2. On the other hand, Bender and co-workers had performed the kinetic decomposition study on mono- and dicationic imidazolium-based ILs coupled with the  $\text{Br}^-$  anion by using the FWO method [28]. It was determined that the values of kinetic parameters for their imidazolium-based dicationic ILs at  $\alpha = 0.1$  and  $\alpha = 0.5$  are higher than our dicationic pyrrolidinium ILs. This indicates that the energy needed by dicationic imidazolium-based ILs for their reactants to reach the transition state is higher than the dicationic pyrrolidinium-based ILs.

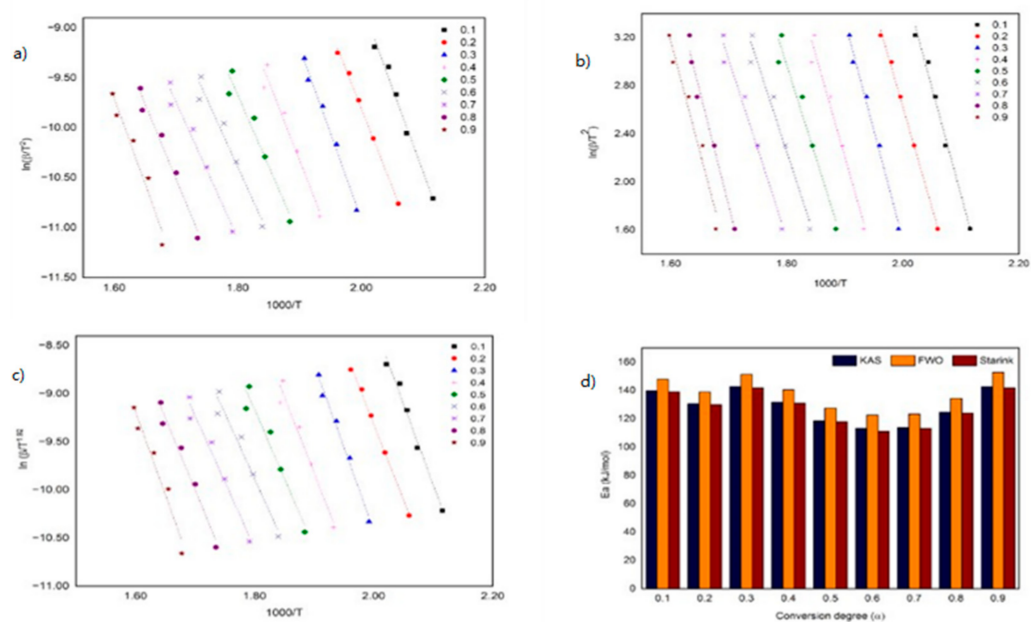


**Figure 5.** Thermokinetic plot using (a) KAS, (b) FWO, (c) Starink method and (d) the  $E_a$  profile for  $[\text{BisC}_4\text{MPyr}][\text{Br}_2]$ .

Data on the maximum operation temperature (MOT) for pyrrolidinium-based ILs are still scarce. Several recent studies used MOT to predict the long-term thermal stability successfully in several recent studies [36–38]. Furthermore, the thermal stability of the ILs mixture is predicted using MOT [39]. The values of the kinetic parameters obtained from this work can be utilized to predict the MOT of ILs. The MOT of  $[\text{C}_4\text{MPyr}][\text{Br}]$  and  $[\text{BisC}_4\text{MPyr}][\text{Br}_2]$  was calculated based on Equation (4), as follows [40]:

$$MOT = \frac{E_a/R}{4.6 + \ln(A \cdot t_{max})} \quad (4)$$

where  $t_{max}$  is the maximum time of exposition. Table 3 shows the MOT of  $[\text{C}_4\text{MPyr}][\text{Br}]$  and  $[\text{BisC}_4\text{MPyr}][\text{Br}_2]$  that was calculated by using kinetic parameters obtained from KAS, FWO and Starink.

**Table 3.** The MOT for [C<sub>4</sub>MPyr][Br] and BisC<sub>4</sub>MPyr][Br<sub>2</sub>].

Methods	[C <sub>4</sub> MPyr][Br]/°C	[BisC <sub>4</sub> MPyr][Br <sub>2</sub> ]/°C
KAS	409.73	398.29
FWO	400.73	375.67
Starink	435.42	423.68

#### 4. Conclusions

This work aims to investigate the thermal stability,  $E_a$  and  $\log A$ , for monocationic and dicationic pyrrolidinium-based ILs. The experimental data on thermal stability indicates low thermal stability of dicationic [BisC<sub>4</sub>MPyr][Br<sub>2</sub>] compared to the monocationic [C<sub>4</sub>MPyr][Br]. The DTG analysis had also revealed the single and multistage decomposition of [C<sub>4</sub>MPyr][Br] and [BisC<sub>4</sub>MPyr][Br<sub>2</sub>], respectively. Furthermore, the kinetic evaluation work was conducted using the KAS, FWO and Starink method, in which the value of  $R^2$  obtained is more than 0.9, thus proving that each  $\alpha$  is best fitted with all the selected kinetic equations. Based on the TG data analysis, it can be concluded that the IL thermal stability does provide a great influence on the  $E_a$  and  $\log A$  values. It was determined that the  $E_a$  and  $\log A$  are linearly proportional with thermal stability of the ILs. In the meantime, while the average values of  $E_a$  for [C<sub>4</sub>MPyr][Br], obtained by using KAS, FWO and Starink, are  $191 \pm 38$ ,  $201 \pm 38$  and  $190 \pm 38$  kJ/mol, the average [BisC<sub>4</sub>MPyr][Br<sub>2</sub>]  $E_a$  are  $129 \pm 12$ ,  $138 \pm 12$  and  $128 \pm 12$  kJ/mol. The same case was also observed in terms of the  $\log A$  value for both ILs. However, the  $E_a$  and  $\log A$  value provided by the FWO model was found to be 10% higher than KAS and Starink, thus suggesting it was quite unreliable. The utilization of the monocationic [C<sub>4</sub>MPyr][Br] and dicationic [BisC<sub>4</sub>MPyr][Br<sub>2</sub>] as catalysts in transesterification has not yet been explored. Therefore, this study is crucial in order to provide preliminary information related to the thermal stability and kinetic property of pyrrolidinium-based ILs as a catalyst.

**Supplementary Materials:** The following supporting information can be downloaded at: <https://www.mdpi.com/article/10.3390/ma15031247/s1>, Table S1: Average temperature of [C<sub>4</sub>MPyr][Br] at each  $\alpha$  value of thermal kinetic decomposition; Table S2: Average temperature of [BisC<sub>4</sub>MPyr][Br] at each  $\alpha$  value thermal kinetic decomposition.

**Author Contributions:** Conceptualization, N.A.G. and N.M.Y.; data curation, N.H. and A.H.A.R.; methodology, N.H., A.H.A.R. and N.S.A.; formal analysis, N.H. and A.H.A.R.; funding acquisition, N.A.G.; project administration, N.A.G. and N.H.; writing—original draft, N.H. and A.H.A.R.; writing—review and editing, N.A.G. All authors have read and agreed to the published version of the manuscript.

**Funding:** This research was funded by Yayasan Universiti Teknologi PETRONAS (YUTP), grant number 015LC-049.

**Institutional Review Board Statement:** Not applicable.

**Informed Consent Statement:** Not applicable.

**Data Availability Statement:** The data that support the findings in the present study are available from the corresponding author upon request.

**Acknowledgments:** Facilities support from Universiti Teknologi PETRONAS and Centre of Research in Ionic Liquids (CORIL), UTP, are greatly acknowledged.

**Conflicts of Interest:** The authors declare no conflict of interest.

#### References

1. Welton, T. Ionic liquids: A brief history. *Biophys. Rev.* **2018**, *10*, 691–706. [[CrossRef](#)]
2. Hurley, F.H.; Wier, T.P., Jr. Electrodeposition of metals from fused quaternary ammonium salts. *J. Electrochem. Soc.* **1951**, *98*, 203. [[CrossRef](#)]

3. Robinson, J.; Osteryoung, R. An electrochemical and spectroscopic study of some aromatic hydrocarbons in the room temperature molten salt system aluminum chloride-n-butylpyridinium chloride. *J. Am. Chem. Soc.* **1979**, *101*, 323–327. [[CrossRef](#)]
4. Dharaskar, S.A.; Varma, M.N.; Shende, D.Z.; Yoo, C.K.; Wasewar, K.L. Synthesis, characterization and application of 1-butyl-3-methylimidazolium chloride as green material for extractive desulfurization of liquid fuel. *Sci. World J.* **2013**, *2013*, 395274. [[CrossRef](#)]
5. Greer, A.J.; Jacquemin, J.; Hardacre, C. Industrial Applications of Ionic Liquids. *Molecules* **2020**, *25*, 5207. [[CrossRef](#)] [[PubMed](#)]
6. Wang, B.; Qin, L.; Mu, T.; Xue, Z.; Gao, G. Are ionic liquids chemically stable? *Chem. Rev.* **2017**, *117*, 7113–7131. [[CrossRef](#)]
7. Dong, K.; Zhang, S.; Wang, J. Understanding the hydrogen bonds in ionic liquids and their roles in properties and reactions. *Chem. Commun.* **2016**, *52*, 6744–6764. [[CrossRef](#)] [[PubMed](#)]
8. Xu, C.; Cheng, Z. Thermal Stability of Ionic Liquids: Current Status and Prospects for Future Development. *Processes* **2021**, *9*, 337. [[CrossRef](#)]
9. Xue, Z.; Qin, L.; Jiang, J.; Mu, T.; Gao, G. Thermal, electrochemical and radiolytic stabilities of ionic liquids. *Phys. Chem. Chem. Phys.* **2018**, *20*, 8382–8402. [[CrossRef](#)]
10. Cao, Y.; Mu, T. Comprehensive investigation on the thermal stability of 66 ionic liquids by thermogravimetric analysis. *Ind. Eng. Chem. Res.* **2014**, *53*, 8651–8664. [[CrossRef](#)]
11. Sbirrazzuoli, N. Interpretation and physical meaning of kinetic parameters obtained from isoconversional kinetic analysis of polymers. *Polymers* **2020**, *12*, 1280. [[CrossRef](#)] [[PubMed](#)]
12. Al-Sallami, W.; Parsaeian, P.; Neville, A. An appraisal of the thermal decomposition mechanisms of ILs as potential lubricants. *Lubr. Sci.* **2019**, *31*, 229–238. [[CrossRef](#)]
13. Akcay, A.; Balci, V.; Uzun, A. Structural Factors Controlling Thermal Stability of Imidazolium Ionic Liquids with 1-n-butyl-3-methylimidazolium cation on  $\gamma$ -Al<sub>2</sub>O<sub>3</sub>. *Thermochim. Acta* **2014**, *589*, 131–136. [[CrossRef](#)]
14. Anderson, J.L.; Ding, R.; Ellern, A.; Armstrong, D.W. Structure and properties of high stability geminal dicationic ionic liquids. *J. Am. Chem. Soc.* **2005**, *127*, 593–604. [[CrossRef](#)]
15. Masri, A.N.; MI, A.M.; Leveque, J.-M. A review on dicationic ionic liquids: Classification and application. *Ind. Eng. Manag.* **2016**, *5*, 197–204.
16. Shirota, H.; Mandai, T.; Fukazawa, H.; Kato, T. Comparison between dicationic and monocationic ionic liquids: Liquid density, thermal properties, surface tension, and shear viscosity. *J. Chem. Eng. Data* **2011**, *56*, 2453–2459. [[CrossRef](#)]
17. Medjahed, N.; Debdab, M.; Haddad, B.; Belarbi, E.; KIBOU, Z.; Berrichi, A.; Bachir, R.; Choukchou-Braham, N. Synthesis and Structural Characterization of Imidazolium-Based Dicationic Ionic Liquids. *Chem. Proc.* **2021**, *3*, 80. [[CrossRef](#)]
18. Qi, M.; Armstrong, D.W. Dicationic ionic liquid stationary phase for GC-MS analysis of volatile compounds in herbal plants. *Anal. Bioanal. Chem.* **2007**, *388*, 889–899. [[CrossRef](#)]
19. Boumediene, M.; Haddad, B.; Paolone, A.; Assenine, M.A.; Villemin, D.; Rahmouni, M.; Bresson, S. Synthesis, conformational studies, vibrational spectra and thermal properties, of new substituted dicationic based on biphenylenedimethylene linked bis-1-methylimidazolium ionic liquids. *J. Mol. Struct.* **2020**. [[CrossRef](#)]
20. Khan, A.S.; Man, Z.; Bustam, M.A.; Kait, C.F.; Ullah, Z.; Sarwono, A.; Wilfred, C.D. Pyrolysis kinetics of 1-propyronitrile imidazolium trifluoroacetate ionic liquid using thermogravimetric analysis. *Procedia Eng.* **2016**, *148*, 1332–1339. [[CrossRef](#)]
21. Muhammad, A. Thermal and kinetic analysis of pure and contaminated ionic liquid: 1-butyl-2,3-dimethylimidazolium chloride (BDMIMCl). *Pol. J. Chem. Technol.* **2016**, *18*, 122–125. [[CrossRef](#)]
22. Quraishi, K.S.; Bustam, M.A.; Krishnan, S.; Aminuddin, N.F.; Azeezah, N.; Ghani, N.A.; Uemura, Y.; Lévêque, J.M. Ionic liquids toxicity on fresh water microalgae, *Scenedesmus quadricauda*, *Chlorella vulgaris* & *Botryococcus braunii*; selection criterion for use in a two-phase partitioning bioreactor (TPPBR). *Chemosphere* **2017**, *184*, 642–651. [[PubMed](#)]
23. Lombardo, M.; Easwar, S.; Pasi, F.; Trombini, C.; Dhavale, D.D. Protonated arginine and lysine as catalysts for the direct asymmetric aldol reaction in ionic liquids. *Tetrahedron* **2008**, *64*, 9203–9207. [[CrossRef](#)]
24. Burrell, A.K.; Del Sesto, R.E.; Baker, S.N.; McCleskey, T.M.; Baker, G.A. The large scale synthesis of pure imidazolium and pyrrolidinium ionic liquids. *Green Chem.* **2007**, *9*, 449–454. [[CrossRef](#)]
25. Montalbán, M.G.; Collado-González, M.; Díaz-Baños, F.G.; Vllora, G. Predicting Density and Refractive Index of Ionic Liquids. In *Ionic Liquids: Progress and Developments in*; IntechOpen Limited: London, UK, 2017; p. 339.
26. Masri, A.; Mutalib, M.A.; Yahya, W.; Aminuddin, N.; Leveque, J. Thermokinetics of SO<sub>3</sub>H-functionalized dicationic ionic liquids: Effect of anions. *IOP Conf. Ser. Mater. Sci. Eng.* **2018**, *458*, 012072. [[CrossRef](#)]
27. Meng, J.; Pan, Y.; Yang, F.; Wang, Y.; Zheng, Z.; Jiang, J. Thermal Stability and Decomposition Kinetics of 1-Alkyl-2,3-Dimethylimidazolium Nitrate Ionic Liquids: TGA and DFT Study. *Materials* **2021**, *14*, 2560. [[CrossRef](#)] [[PubMed](#)]
28. Bender, C.R.; Kuhn, B.L.; Farias, C.A.; Ziembowicz, F.I.; Beck, T.S.; Frizzo, C.P. Thermal Stability and Kinetic of Decomposition of Mono-and Dicationic Imidazolium-Based Ionic Liquids. *J. Braz. Chem. Soc.* **2019**, *30*, 2199–2209. [[CrossRef](#)]
29. Fareghi-Alamdari, R.; Ghorbani-Zamania, F.; Shekarriz, M. Synthesis and thermal characterization of mono and dicationicimidazolium-pyridinium based ionic liquids. *Orient. J. Chem.* **2015**, *31*, 1127. [[CrossRef](#)]
30. Guglielmero, L.; Mezzetta, A.; Guazzelli, L.; Pomelli, C.S.; D'Andrea, F.; Chiappe, C. Systematic synthesis and properties evaluation of dicationic ionic liquids, and a glance into a potential new field. *Front. Chem.* **2018**, *6*, 612. [[CrossRef](#)] [[PubMed](#)]
31. Al-Moftah, A.M.S.; Marsh, R.; Steer, J. Thermal decomposition kinetic study of non-recyclable paper and plastic waste by thermogravimetric analysis. *ChemEngineering* **2021**, *5*, 54. [[CrossRef](#)]

32. Chen, Y.; Mu, T. Thermal Stability of Ionic Liquids. In *Encyclopedia of Ionic Liquids*; Zhang, S., Ed.; Springer: Singapore, 2019; pp. 1–13. [[CrossRef](#)]
33. Patil, R.A.; Talebi, M.; Berthod, A.; Armstrong, D.W. Dicationic ionic liquid thermal decomposition pathways. *Anal. Bioanal. Chem.* **2018**, *410*, 4645–4655. [[CrossRef](#)]
34. Wooster, T.J.; Johanson, K.M.; Fraser, K.J.; MacFarlane, D.R.; Scott, J.L. Thermal degradation of cyano containing ionic liquids. *Green Chem.* **2006**, *8*, 691–696. [[CrossRef](#)]
35. Guida, M.; Lanaya, S.; Rbihi, Z.; Hannioui, A. Thermal degradation behaviors of sawdust wood waste: Pyrolysis kinetic and mechanism. *J. Mater. Environ. Sci.* **2019**, *10*, 742–755.
36. Jiang, H.-C.; Lin, W.-C.; Hua, M.; Pan, X.-H.; Shu, C.-M.; Jiang, J.-C. Analysis of thermal stability and pyrolysis kinetic of dibutyl phosphate-based ionic liquid through thermogravimetry, gas chromatography/mass spectrometry, and Fourier transform infrared spectrometry. *J. Therm. Anal. Calorim.* **2019**, *138*, 489–499. [[CrossRef](#)]
37. Efimova, A.; Pfützner, L.; Schmidt, P. Thermal stability and decomposition mechanism of 1-ethyl-3-methylimidazolium halides. *Thermochim. Acta* **2015**, *604*, 129–136. [[CrossRef](#)]
38. Parajo, J.; Villanueva, M.; Troncoso, J.; Salgado, J. Thermophysical properties of choline and pyridinium based ionic liquids as advanced materials for energy applications. *J. Chem. Thermodyn.* **2020**, *141*, 105947. [[CrossRef](#)]
39. Navarro, P.; Larriba, M.; García, J.; Rodríguez, F. Thermal stability and specific heats of {[emim][DCA]}+[emim][TCM]} mixed ionic liquids. *Thermochim. Acta* **2014**, *588*, 22–27. [[CrossRef](#)]
40. Parajó, J.J.; Villanueva, M.; Salgado, J. 1. Thermal stability of ionic liquids. In *Ionic Liquids: Synthesis, Properties, Technologies and Applications*; Rasmus, F., Catherine, S., Eds.; De Gruyter: Berlin, Germany, 2019; pp. 1–16. [[CrossRef](#)]